THE JOURNAL OF
PHYSICAL CHEMISTRY

Subscriber access provided by University of Texas Libraries

# Photochemistry of tris(2,2'-bipyridyl)(ruthenium(II) in colloidal clay suspensions

Pushpito K. Ghosh, and Allen J. Bard

*J. Phys. Chem.*, **1984**, 88 (23), 5519-5526• DOI: 10.1021/j150667a012 • Publication Date (Web): 01 May 2002

**Downloaded from http://pubs.acs.org on February 12, 2009**

## More About This Article

The permalink http://dx.doi.org/10.1021/j150667a012 provides access to:

- Links to articles and content related to this article
- Copyright permission to reproduce figures and/or text from this article

ACS Publications
High quality. High impact.

The Journal of Physical Chemistry is published by the American Chemical Society.
1155 Sixteenth Street N.W., Washington, DC 20036

complexes the indole chromophore was found to be the proton-donating substituent. The spectral shifts of these complexes, and thus the relative strength of the hydrogen bond, are shown to give a reasonable linear correlation with the basicities of the partners as measured by the respective proton affinities. This correlation was also found to hold in general for substituted indoles. The use of the gas-phase proton affinity, which has previously been found to be sensitive to the polarizability of the attached alkyl groups, has made it possible to compare the important interaction components in terms of Morokuma's energy decomposition analysis. We have interpreted the ordering of indole hydrogen-bonded spectral shifts in terms of the interplay of both electrostatic interaction and polarization interaction components. It appears that for weakly bonded systems such as those containing indole as the proton donor, polarization forces can become important in determining electronic spectral shifts.

We have also shown that indole and species such as halocarbons that are important in anesthetic activity can participate in hydrogen bonds where the indole moiety is the proton acceptor. This observation provides a unique opportunity to investigate the dynamics of such biological processes in an isolated environment. Further investigations on these hydrogen-bonded indoles are currently in progress in our laboratory.

*Acknowledgment.* The financial support of the Natural Sciences and Engineering Research Council of Canada and the Petroleum Research Fund, administered by the American Chemical Society, is gratefully acknowledged. We wish to thank Dr. R. Houriet for providing us with unpublished values of proton affinities and Prof. A. G. Harrison for helpful discussions.

**Registry No.** $H_2O$, 7732-18-5; MeOH, 67-56-1; EtOH, 64-17-5; 1-PrOH, 71-23-8; 2-PrOH, 67-63-0; 1-BuOH, 71-36-3; $NH_3$, 7664-41-7; $N(Me)_3$, 75-50-3; $(i\text{-Pr})_2NH$, 108-18-9; $HCCl_3$, 67-66-3; $H_2CCl_2$, 75-09-2; benzene, 71-43-2; 1,4-dioxane, 123-91-1; indole, 120-72-9; 5-methylindole, 614-96-0; 5-methoxyindole, 1006-94-6; 7-methylindole, 933-67-5.

# Photochemistry of Tris(2,2′-bipyridyl)ruthenium(II) in Colloidal Clay Suspensions

**Pushpito K. Ghosh and Allen J. Bard***

*Department of Chemistry, The University of Texas, Austin, Texas 78712* *(Received: May 31, 1984)*

The spectroscopy (absorption, emission, and resonance Raman), photophysics, and photochemistry of $Ru(bpy)_3^{2+}$ (bpy is 2,2′-bipyridine) in colloidal smectites have been studied. The structure of $Ru(bpy)_3^{2+}$ is shown to remain relatively unperturbed in the adsorbed state. The clay interlayers segregate $Ru(bpy)_3^{2+}$ from exchangeable $Na^+$ ions, resulting in high local concentrations of the complex cations in the interlayer. This in turn leads to very efficient excited-state self-quenching processes (60% of the initially formed $Ru(bpy)_3^{2+*}$ decays with an average lifetime of 55 ns when as little as 7% of the molecules are excited) under normal pulsed laser conditions. $Ru(bpy)_3^{2+}$ also segregates from $MV^{2+}$ (methylviologen) in the interlayer, leading to poor efficiencies for the quenching of the excited state by adsorbed $MV^{2+}$ compared to that in homogeneous solution. The excited state is readily quenched, however, by the neutral viologen, PVS (propylviologen sulfonate). In contrast to the segregation from $Na^+$ and $MV^{2+}$, $Ru(bpy)_3^{2+}$ randomly mixes with $Zn(bpy)_3^{2+}$ in the interlayer, as evidenced by the progressive decrease in excited-state self-quenching rate for increasing ratios of $[Zn(bpy)_3^{2+}]:[Ru(bpy)_3^{2+}]$.

## Introduction

Clays constitute a unique class of inorganic colloids with special structural features that make them versatile as catalysts[1] and catalyst supports.[2] Of special interest are the swelling phyllosilicate minerals known as smectite clays. The smectites (e.g., hectorite, montmorillonite) can be readily dispersed in water, possess a large surface area (~750 $m^2/g$), have a very high cation-exchange capacity (~100 mequiv/100 g), and exhibit unusual intercalation and swelling properties. Recently we described the electrochemistry of several different ions confined to electrode surfaces modified with such a clay.[3] It is of interest in connection with such clay-modified electrodes to investigate how ions from solution are incorporated into such clays. In the work described here we report our observations on the spectroscopy and photochemistry of $Ru(bpy)_3^{2+}$ in colloidal suspensions of sodium hectorite and sodium montmorillonite. Due to its unique ground- and excited-state properties[4–11] the photochemistry of $Ru(bpy)_3^{2+}$ in clay suspensions is of considerable interest.[12] In addition, its possible use as a pillaring agent (molecular prop) in smectites has also been discussed.[13] We have obtained absorption and emission data for absorbed $Ru(bpy)_3^{2+}$ and have probed its structure by resonance Raman spectroscopy. We have also used the techniques of laser flash photolysis and time-correlated single-photon counting to obtain emission decay profiles of $Ru(bpy)_3^{2+}$ in the adsorbed state. We assign the efficient self-quenching to triplet–triplet annihilation under normal (high-in-

(1) (a) Weiss, A. *Angew. Chem., Int. Ed. Engl.* **1981**, *20*, 850. (b) Shimoyama, A.; Johns, W. D. *Nature (London), Phys. Sci.* **1971**, *232*, 140. (c) Durand, B.; Fripiat, J. J.; Pelet, R. *Clays Clay Miner.* **1972**, *20*, 21.
(2) Van Olphen, H. "An Introduction to Clay Colloid Chemistry"; Wiley: New York, 1977.
(3) Ghosh, P. K.; Bard, A. J. *J. Am. Chem. Soc.* **1983**, *105*, 5691.
(4) Demas, J. N.; Crosby, G. A. *J. Mol. Spectrosc.* **1968**, *26*, 72.
(5) Lyte, F. E.; Hercules, D. M. *J. Am. Chem. Soc.* **1969**, *91*, 72.
(6) Demas, J. N.; Adamson, A. W. *J. Am. Chem. Soc.* **1973**, *95*, 5159.
(7) (a) Navon, G.; Sutin, N. *Inorg. Chem.* **1974**, *13*, 2159. (b) Sutin, N.; Creutz, C. *Adv. Chem. Ser. No.* **1978**, *168*, 1. (c) This single-exponential decay in good agreement with previous work indicates that the more complex behavior found with clays cannot be attributed to impurities in the $Ru(bpy)_3Cl_2$ sample.
(8) (a) Laurence, G. S.; Balzani, V. *Inorg. Chem.* **1974**, *13*, 3663. (b) Balzani, V.; Bolletta, F.; Gandolfi, M. R.; Maestri, M. *Top. Curr. Chem.* **1978**, *75*, 1.
(9) Young, R. C.; Keene, F. R.; Meyer, T. J. *J. Am. Chem. Soc.* **1977**, *99*, 2468.
(10) Bock, C. R.; Meyer, T. J.; Whitten, D. G. *J. Am. Chem. Soc.* **1974**, *96*, 4710.
(11) (a) Harrigan, R. W.; Hager, G. D.; Crosby, G. A. *Chem. Phys. Lett.* **1973**, *21*, 487. (b) Hager, G. D.; Crosby, G. A. *J. Am. Chem. Soc.* **9175**, *97*, 7031.
(12) (a) Nijs, H.; Fripiat, J. J.; Van Damme, H. *J. Phys. Chem.* **1983**, *87*, 1279. (b) Nijs, H.; Cruz, M. I.; Fripiat, J. J.; Van Damme, H., *J. Chem. Soc. Chem. Commun.* **1981**, *1026*.
(13) Pinnavaia, T. J. *Science (Washington, D.C.)* **1983**, *220*, 365.

0022-3654/84/2088-5519$01.50/0 © 1984 American Chemical Society

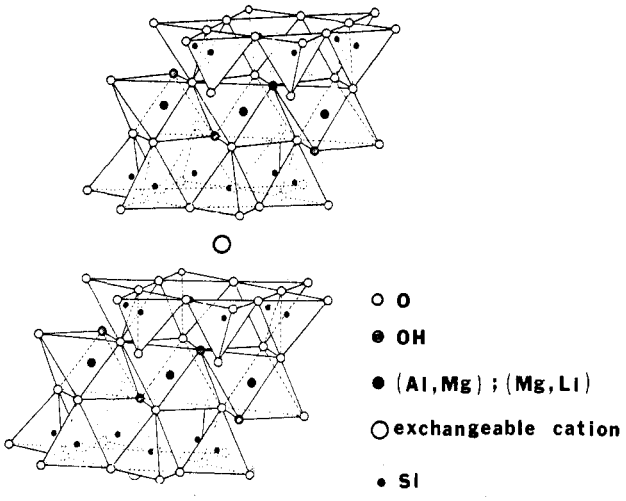


**Figure 1.** Schematic structure of 2:1 layer silicates (smectites).

tensity) pulsed laser conditions. In conjunction with observations from quenching studies using viologens, our results highlight some of the remarkable intercalation properties of smectites. We note that $Ru(bpy)_3^{2+}$ has been previously used as a luminescent probe in clay films and colloidal clay suspensions.[14,15]

## Experimental Section

*Materials.* $Ru(bpy)_3Cl_2$ was purchased from G. F. Smith and recrystallized from hot water. Methylviologen ($MV^{2+}$) hydrate was procured from Aldrich Chemical Co. $Zn(bpy)_3Cl_2$[16] and propylviologen sulfonate[17] (PVS) were synthesized according to published procedures. Calcium hectorite and Wyoming bentonite were provided by the Clay Minerals Repository, while the low-iron montmorillonite (GK 129) was a generous gift from the Georgia Kaolin Co. All clays were converted to the $Na^+$-exchanged form by stirring in 1 M NaCl for 3–4 days. They were subsequently purified by repeated cycles of centrifugation followed by suspension in triply distilled water. The suspensions were finally centrifuged at 9000 rpm and the supernatants dialyzed to remove excess chloride ions. The clay concentrations in these colloidal dispersions following the above treatment were typically 6–10 g/L.

*Instrumentation.* Absorption spectra were recorded on either a Hewlett-Packard 8450 or Cary 17 A spectrophotometer and emission spectra were recorded on an Aminco-Bowman spectrophotofluorimeter with a Hamamatsu R 928 photomultiplier tube. Resonance Raman spectra were obtained by excitation with the 457.9-nm line of a Spectra Physics continuous-wave $Ar^+$ laser. Details of the experimental setup have been reported previously.[18] Fluorescence lifetimes under low light intensity were obtained by using time-correlated single-photon counting on a PRA fluorescence lifetime instrument with an Apple II plus microcomputer for data acquisition and data reduction. The excitation source was the 337-nm line of a triggered $N_2$ lamp. Emission lifetimes under high light intensity were obtained by using a Quantel YG 481 Nd:YAG laser having a ca. 12-ns pulse or the 200-ps pulse from a Quantel YG 402 mode-locked Nd:YAG laser as the excitation source. The 355-nm line was most commonly used, but the 450-nm line from a Quantel TDL III dye laser (Coumarin 450) was also employed in some experiments. The emission signals were collected with a conventional monochromator/photomultiplier setup with appropriate filters to eliminate scattered laser light. Signals were digitized in a Tetronix 7912 transient recorder and analyzed on line by a PDP-11/70 computer. Typically 5–10 shots were signal averaged prior to kinetic analysis.

## Results and Discussion

The structure of the phyllosilicates is shown in Figure 1. Each sheet consists of two inverted tetrahedral layers sharing their apical oxygen with an octahedral layer. While the tetrahedral layers are generally silicate sheets, different ions can be found in the octahedral layer. The electroneutral mineral pyrophyllite has two out of three octahedral sites occupied by Al(III), while in talc, all three octahedral sites are occupied by Mg(II). Substitution of ~15% Al(III) with Mg(II) and ~8% Mg(II) with Li(I) results in the commonly observable structures of montmorillonite and hectorite, respectively. The cation-exchange capacity originates from a lack of electroneutrality in these clays. Small quantities of other ions such as Fe(III), Fe(II), etc., may also be present in the octahedral sites and can significantly affect the luminescence behavior of $Ru(bpy)_3^{2+}$.[14] The phyllosilicate sheets are stacked together in the solid state (presumably due to van der Waals interaction), but tend to break apart into isolated platelets when suspended in water. However, this delamination process is not complete.[19] Consequently, exchangeable cations can reside on the outer surface as well as be intercalated between sheets. Using photon correlation spectroscopy, we have obtained an effective spherical diameter of 0.22 $\mu$m for the colloidal particles. Although this does not give us the actual dimensions of the clay particles, which are rectangular platelets, we presume that there are at least 3–5 sheets/particle.

*Absorbance and Emission of Clay/Ru(bpy)$_3^{2+}$.* In Figure 2 we have compiled some of the spectral features for $Ru(bpy)_3^{2+}$ in water and in finely dispersed suspensions of sodium hectorite and sodium montmorillonite. By centrifuging the suspensions at high speed (30 000 rpm) we have determined that essentially all the $Ru(bpy)_3^{2+}$ is adsorbed in the clay, since no $Ru(bpy)_3^{2+*}$ emission is observed from the supernatant liquid. As shown in Figure 2a, the charge-transfer absorption band for adsorbed $Ru(bpy)_3^{2+}$ is shifted toward the red $\tau_{max}$ ~ 470 nm) with an increased absorption cross section ($\epsilon_{470}$ = 21000 $M^{-1}$ $cm^{-1}$ in clay vs. $\epsilon_{450}$ = 14500 $M^{-1}$ $cm^{-1}$ in water). One other notable feature not shown in Figure 2a is a split in the $\pi$–$\pi^*$ band around 285 nm when $Ru(bpy)_3^{2+}$ is adsorbed on the colloid. The differences in absorption spectra have been attributed to interactions between $Ru(bpy)_3^{2+}$ and the clay surface.[15] Possible explanations include distortion of the bipyridine ligands due to steric constraints and an enhancement in the quasi metal-to-ligand charge transfer in the ground state. In contrast to the differences in absorption spectra, the luminescence profiles are very similar (Figure 2c). The excitation spectra also essentially track the absorption profiles (Figure 2b). However, there are sizable differences in the relative magnitudes of the luminescence quantum yields. Correcting for changes in absorption cross section, we find that the yield is ~30% larger for $Ru(bpy)_3^{2+}$ in hectorite, whereas it is almost 6 times lower for $Ru(bpy)_3^{2+}$ in montmorillonite. The greatly reduced yield for $Ru(bpy)_3^{2+}$–montmorillonite can be attributed to quenching by Fe(III) present in the octahedral layer. In fact, the emission is completely quenched when $Ru(bpy)_3^{2+}$ is incorporated into Wyoming bentonite, a montomorillonite with high Fe content. Surprisingly, the quantum yield was not increased even after removing Fe by the method of Mehra and Jackson.[20a] We believe this is probably because their treatment only removes free $Fe_2O_3$, but not Fe substituted in the octahedral layer.[20b] The quenching

(14) Krenske, D.; Abdo, S.; Van Damme, H.; Cruz, M.; Fripiat, J. J. *J. Phys. Chem.* **1980**, *84*, 2447.
(15) DellaGuardia, R. A.; Thomas J. K. *J. Phys. Chem.* **1983**, *87*, 990.
(16) Inskeep, R. G. *J. Inorg. Nucl. Chem.* **1962**, *24*, 763.
(17) Maverick, A. W.; Najdzionek, J. S.; Mackenzie, D.; Nocera, D. G.; Gray, H. B. *J. Am. Chem. Soc.* **1983**, *105*, 1878.
(18) Bradley, P. G.; Kress, N.; Hornberger, B. A.; Dallinger, R. F.; Woodruff, W. H. *J. Am. Chem. Soc.* **1981**, *103*, 7441.
(19) Van Olphen, H. "An Introduction to Clay Colloid Chemistry"; Wiley: New York, 1977; Chapter 7.
(20) (a) Mehra, O. P.; Jackson, M. L. *Clays Clay Miner., Proc. Conf.* **1958**, *7*, 317. Briefly, the experimental procedure for removal of iron oxide is as follows: a round-bottom flask containing a well-stirred suspension of wyoming Bentonite (5 g) in a sodium citrate (0.3 M) sodium bicarbonate (0.1 M) solution (200 mL) was heated to 80 °C and sodium dithionite (5 g) was gradually added till the grayish-looking suspension turned white. Following a 15-min digestion period, flocculation was induced by the addition of 50 mL of saturated NaCl and 25 mL of acetone. The suspension was then centrifuged at 2500 rpm and the clay residue was purified by repeated washing with distilled water. (b) That the method of Mehra and Jackson only removes free $Fe_2O_3$ and not Fe in the octahedral lattice has been inferred from the negligible loss in cation-exchange capacity following the above treatment.[20a]

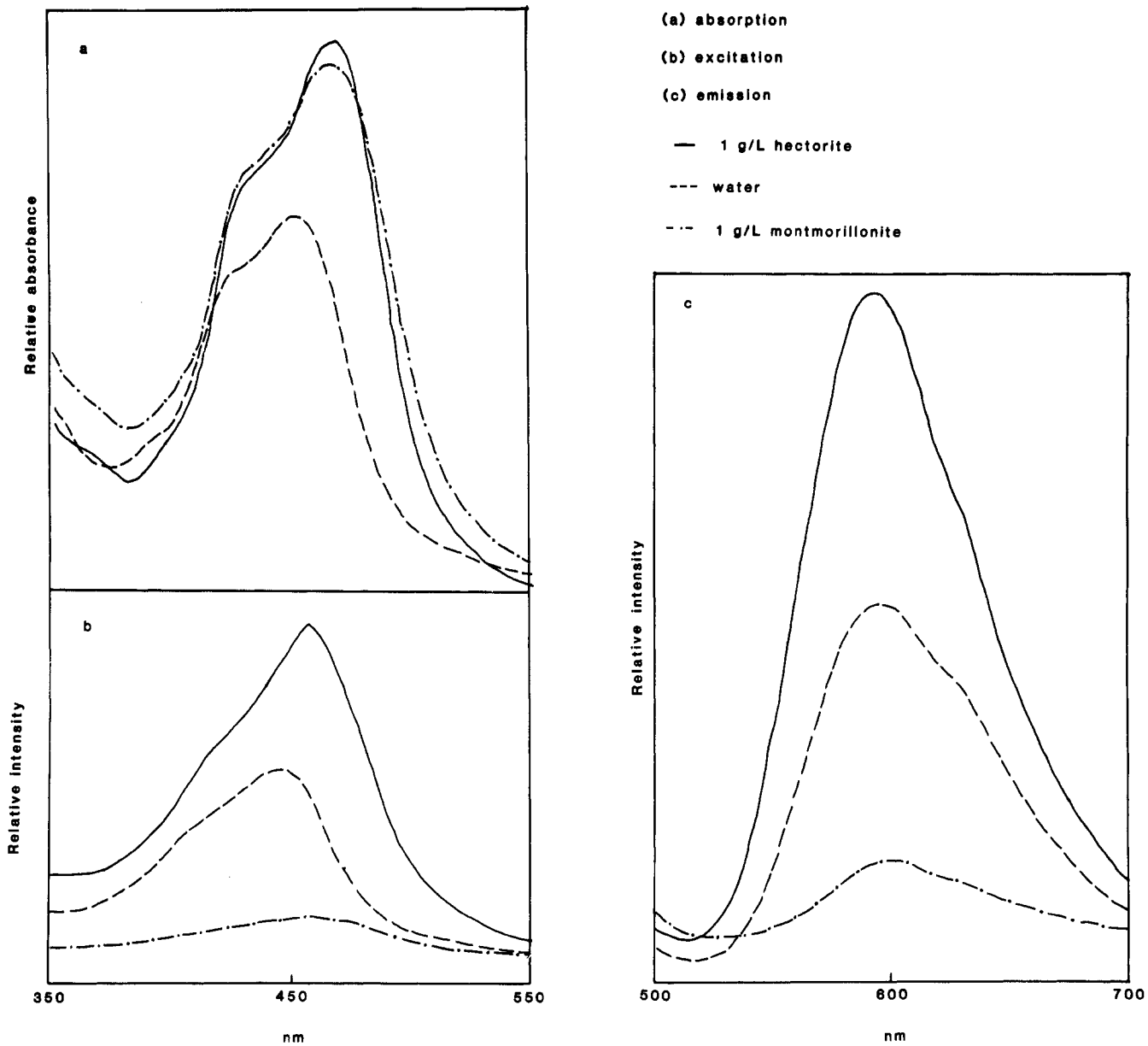


**Figure 2.** (a) Adsorption, (b) excitation, and (c) emission spectra of $2 \times 10^{-5}$ M $Ru(bpy)_3^{2+}$ in water (---), sodium hectorite (—), and sodium montmorillonite (-·-). The absorption spectra were measured vs. the appropriate $Ru(bpy)_3^{2+}$-free solutions in the reference cell. The excitation spectra were recorded by monitoring the emission at 610 nm, while the phosphorescence spectra were obtained by using 460-nm excitation.

by Fe(III) is worth noting especially since the octahedral sites are 4 Å removed from the location of exchangeable cations. Overall, our absorption and emission data are in good agreement with those of Krenske et al.[14] and DellaGuardia and Thomas.[15]

*Resonance Raman Spectra.* An increase in the quasi metal-to-ligand charge transfer in the ground state has been invoked to rationalize the absorption spectral shifts resulting from the adsorption of $Ru(bpy)_3^{2+}$ in clay. That such a charge transfer takes place has been inferred from XPS data for $Ru(bpy)_3^{2+}$ in hectorite films.[21] Unfortunately, we have not been able to reproduce these results. However, resonance Raman spectra of $Ru(bpy)_3^{2+}$ in water and colloidal hectorite (adsorption was confirmed by centrifuging the colloidal suspension) provide little evidence for any such additional ground-state charge transfer. The spectrum in water (Figure 3a) is in reasonable agreement with literature data[18] and it is also very similar to the spectrum obtained in hectorite suspension (Figure 3b). The vibrational features in Figure 3 are due to symmetric C=C and C=N stretches, and these stretching frequencies are sensitive to the charge density on the bpy ligand.[18,22] Therefore, we interpret the lack of spectral shifts as proof against any significant perturbation of the $Ru(bpy)_3^{2+}$ ion.

*Photoluminescence of Clay/$Ru(bpy)_3^{2+}$.* The luminescence decay profile for $2 \times 10^{-5}$ M $Ru(bpy)_3^{2+}$ in colloidal hectorite using 355-nm pulsed laser illumination is given in Figure 4a. While the $Ru(bpy)_3^{2+*}$ in water exhibited a first-order decay ($\tau$ = 550 ns), in good agreement with published results,[7b,c] the emission profile for adsorbed $Ru(bpy)_3^{2+*}$ was considerably more complex. The emission kinetics could be fitted to a double-exponential decay: $\alpha = 0.6$, $\tau = 62$ ns; $1 - \alpha = 0.4$, $\tau = 350$ ns, where $\alpha$ is the fraction of emitter molecules with a particular decay rate, at time zero. Our results are in qualitative agreement with the data of DellaGuardia and Thomas[15] for $Ru(bpy)_3^{2+}$ in montmorillonite. These authors suggested that the double-exponential decay is due to the presence of two different sites on the clay surface. Such a view is possible in light of recent results for $Ru(bpy)_3^{2+}$ in zeolites[23] and silica,[24] and as mentioned above,

(21) Abdo, S.; Canesson, P.; Cruz, M.; Fripiat, J. J.; Van Damme, H. *J. Phys. Chem.* **1981**, *85*, 797.

(22) Dallinger, R. F.; Woodruff, W. H. *J. Am. Chem. Soc.* **1979**, *101*, 1355.

(23) Wilkins, K.; Faulkner, L. R., personal communication.

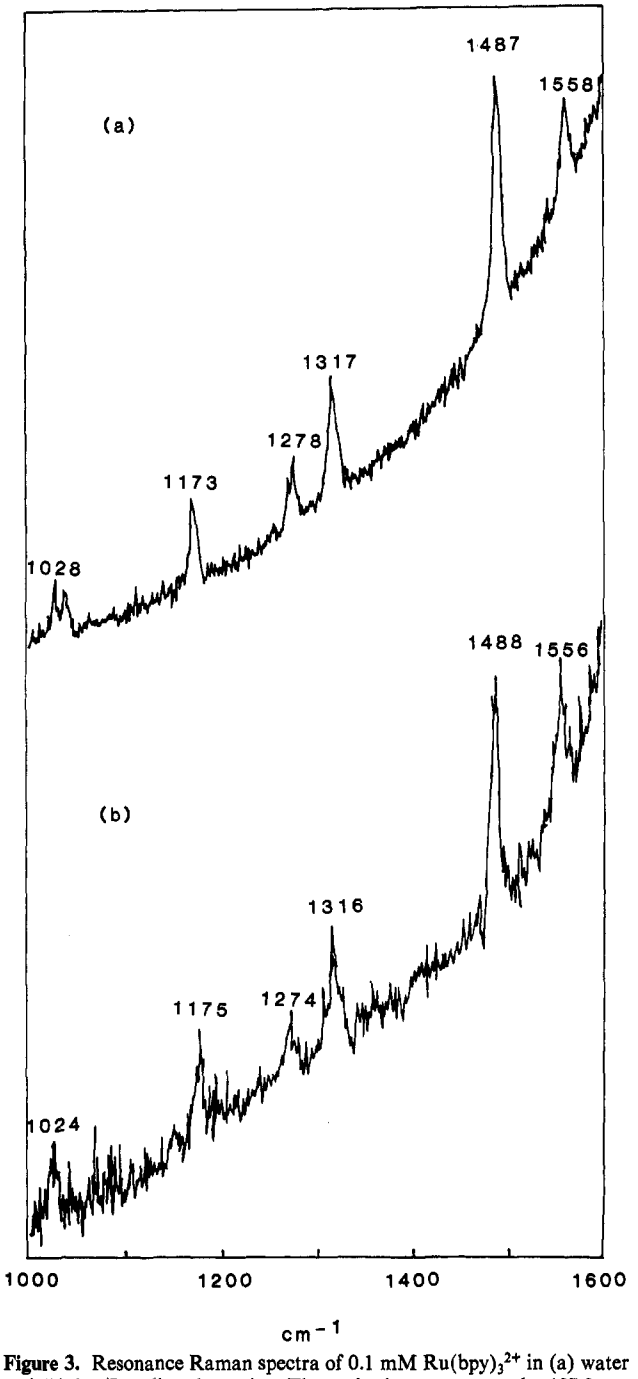


**Figure 3.** Resonance Raman spectra of 0.1 mM $Ru(bpy)_3^{2+}$ in (a) water and (b) 3 g/L sodium hectorite. The excitation source was the 457.9-nm line of the $Ar^+$ continuous-wave laser.

$Ru(bpy)_3^{2+}$ can be present on the outer surfaces of the clay particle as well as be intercalated between phyllosilicate sheets. The enhanced decay rates for $Ru(bpy)_3^{2+*}$ in clay compared to those in homogeneous solutions are more difficult to rationalize, however. DellaGuardia and Thomas suggested that quenching by Fe in the aluminosilicate lattice may be a factor.[15] However, our steady-state emission measurements (Figure 2c) have shown that quenching by Fe is negligible in hectorite; in fact, our emission yield is higher for hectorite-incorporated $Ru(bpy)_3^{2+}$ than that in aqueous solution. Since the principal difference between the steady-state measurements and the pulsed laser experiments is the illumination intensity, we examined the emission decay profile under low-level illumination. The emission profile obtained by using the technique of time-correlated single-photon counting with

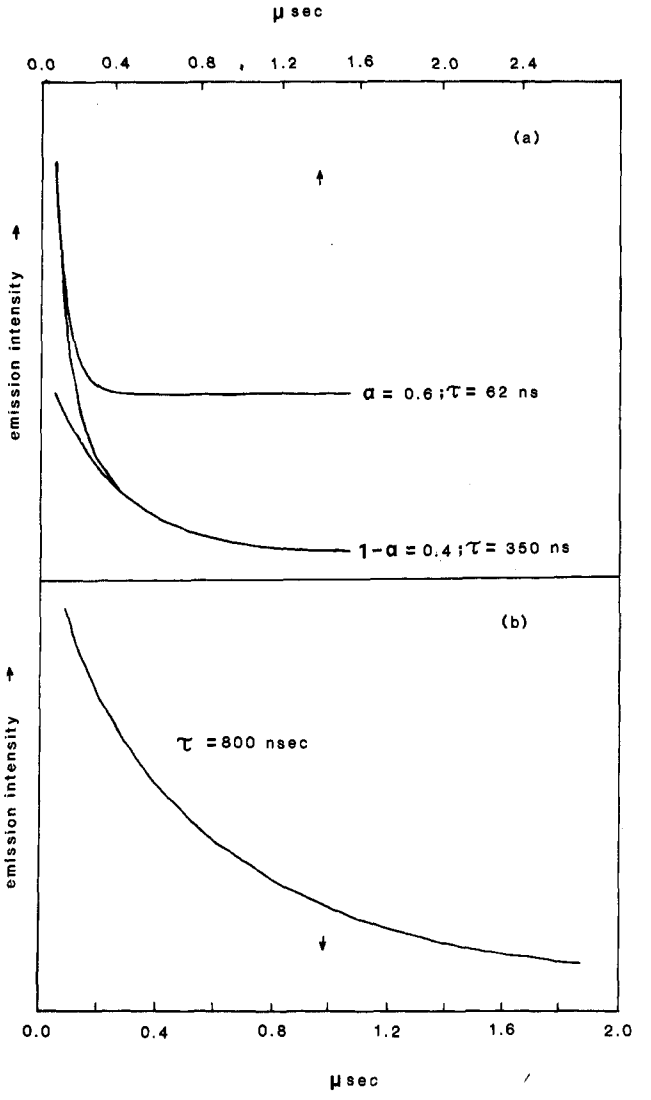


**Figure 4.** Emission decay profiles of $2 \times 10^{-5}$ M $Ru(bpy)_3^{2+}$ in 1 g/L sodium hectorite: (a) high-intensity excitation using picosecond laser (355-nm line) and (b) low-intensity illumination with a triggered $N_2$ lamp (337-nm line).

low-intensity excitation can be fitted to a single-exponential decay with $\tau = 800$ ns.[25] The somewhat longer lifetime compared to that in water is in good accord with the ~30% increase in emission quantum yield for $Ru(bpy)_3^{2+}$ adsorbed in hectorite. These experiments demonstrate that the high light fluxes obtained by using pulsed laser excitation promote self-quenching processes within the clay, resulting in substantially decreased lifetimes of the excited state. Self-quenching by triplet–triplet annihilation has also been observed for $Ru(bpy)_3^{2+}$ in sodium dodecyl sulfate solutions below the critical micelle concentrations.[26,27] While we do not discount the possibility of two different sites on the clay surface, the data in Figure 4b indicate that the radiative lifetimes of $Ru(bpy)_3^{2+*}$ would then have to be similar in these environments.

Since the emission kinetics strongly depend on the illumination intensity, it is inappropriate to analyze the luminescence decay

(24) Kajiwara, T.; Jasimoto, K.; Kawai, T.; Sakata, T. *J. Phys. Chem.* **1982**, *86*, 4516.

(25) Upon completion of this work a report has appeared (Hahti, A.; Keravis, D.; Levitz, P.; Van Damme, H. *J. Chem. Soc., Faraday Trans. 2* **1984**, *80*, 67 on the emission kinetics of $Ru(bpy)_3^{2+}$ in clays under low-level illumination. These authors have observed multiexponential decays in their experiments although lifetimes of all exponentials were longer than 300 ns. Our decay profile could be fitted by a single exponential, except at the very fast time scale ($t < 75$ ns), where small deviations due to biphasic behavior were observed.

(26) Lachish, U.; Ottolenghi, M.; Rabani, J. *J. Am. Chem. Soc.* **1977**, *99*, 8062.

(27) (a) Baxendale, J. H.; Rodgers, M. A. J. *Chem. Phys. Lett.* **1980**, *72*, 424. (b) Baxendale, J. H.; Rodgers, M. A. J. *J. Phys. Chem.* **1982**, *86*, 4906.

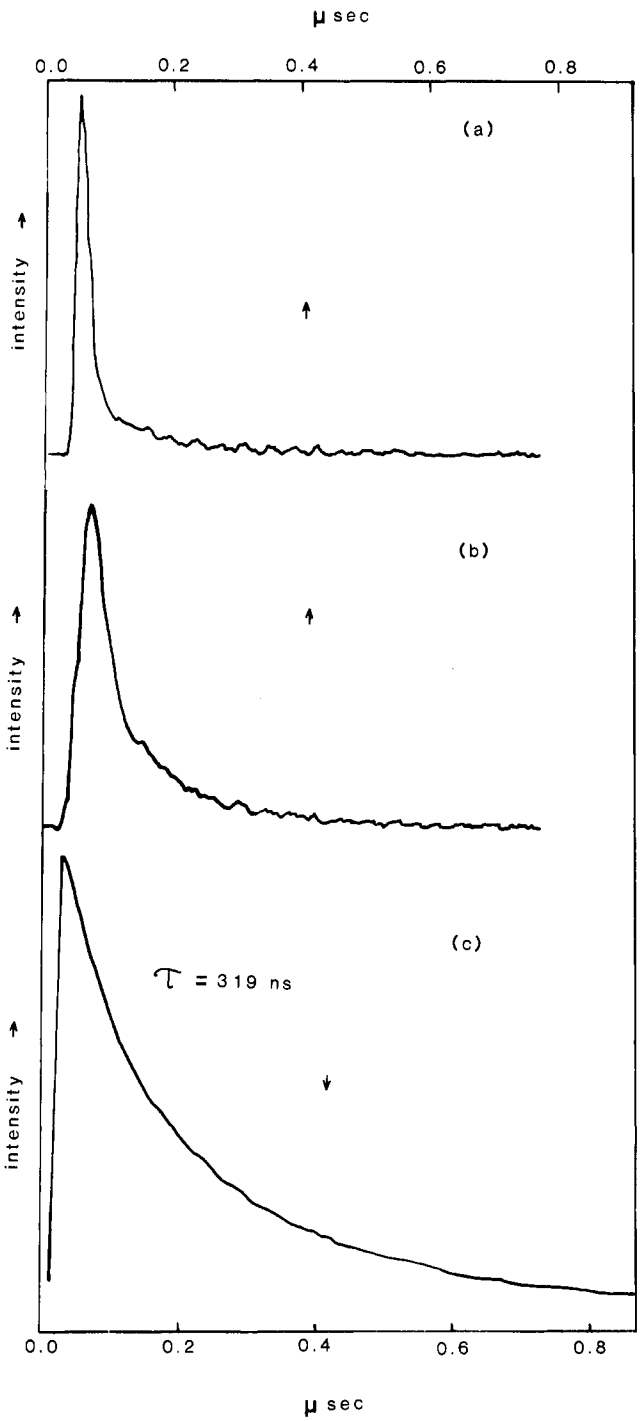


**Figure 5.** Emission decay profiles of $4 \times 10^{-5}$ M $Ru(bpy)_3^{2+}$ in 2.5 g/L sodium montomorillonite: (a) high-intensity excitation using nanosecond pulsed laser (355-nm line), (b) same as a except that the pulse energy was attenuated by a factor of 5–7, (c) low-intensity excitation using a triggered $N_2$ lamp (337-nm line).

profiles by using a double-exponential fitting routine. Nevertheless, such simulations are usful in comparing relative self-quenching rates in different systems under identical illumination conditions. We have used this approach in several instances to be discussed below.

Emission kinetics data for $Ru(bpy)_3^{2+}$ adsorbed in sodium montmorillonite (Figure 5) are in agreement with the lower emission yield reported in Figure 2c; the emission lifetime measured under low light levels is only 319 ns (Figure 5c). This lifetime, however, is still too large to account for the sixfold decrease in luminescence quantum yield. We suspect that this discrepancy is due to significant contributions from static quenching in the steady-state experiments. Illumination with a

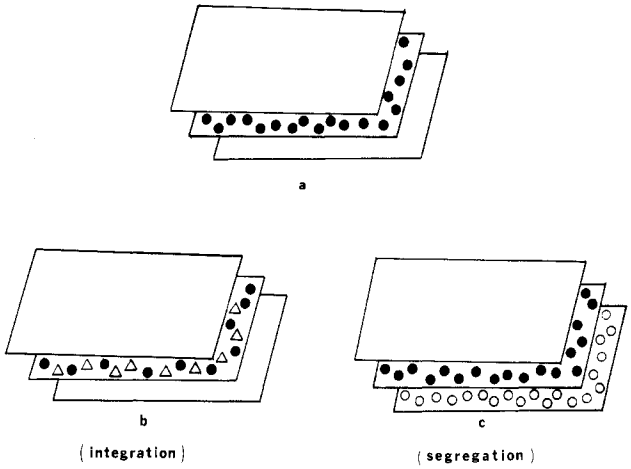


**Figure 6.** Schematics of the different modes of intercalation of exchangeable cations in colloidal sodium hectorite suspensions: (●) $Ru(bpy)_3^{2+}$, (△) $Zn(bpy)_3^{2+}$, (○) $MV^{2+}$. $Na^+$ ions are not shown.

pulsed laser source reveals that self-quenching readily occurs in the $Ru(bpy)_3^{2+}$–montmorillonite system as well.[28] This is apparent from a comparison of the traces in Figure 5, a (high intensity) and b (moderate intensity), with that in Figure 5c (low intensity).

To test whether the self-quenching rate can be varied as a function of the effective concentration of $Ru(bpy)_3^{2+}$ in the clay, we obtained luminescence decay profiles for several [$Ru(bpy)_3^{2+}$]:[clay] ratios. The illumination conditions were maintained constant, the $Ru(bpy)_3^{2+}$ concentration (0.02 mM) was the same in all solutions, and only the clay (hectorite) content (0.25–2.5 g/L) was varied. No serious problem with scattered light was encountered in these experiments. All of the traces were very similar, suggesting that there is little change in the effective concentration of $Ru(bpy)_3^{2+}$ in these clay suspensions even though the clay concentration was varied over a factor of 10. This apparently anomalous behavior can be attributed to ion segregation (i.e., there is a nonrandom distribution of $Ru(bpy)_3^{2+}$ ions in the clay layers). Evidence for such ion segregation has also been found from X-ray diffraction studies on thin films of sodium(I) hectorite containing fractional symmetries of $Fe(phen)_3^{2+}$.[29] These latter results suggest that complete adsorption of $Fe(phen)_3^{2+}$ occurs in a given interlayer before adsorption can occur in succeeding interlayers. In our case such a situation would yield the same concentration of $Ru(bpy)_3^{2+}$ within an interlayer, irrespective of the amount of clay in solution—i.e., a given interlayer would either be completely saturated with $Ru(bpy)_3^{2+}$ or not be occupied at all (see Figure 6a). The large effective concentration of $Ru(bpy)_3^{2+}$ ions resulting from complete occupancy within a layer (Krenske et al. estimate an average distance of ~11.5 Å between ion-exchange sites on the surface[14]) would then help explain the high self-quenching efficiences observed in these systems. Our preliminary experiments suggest that when as little as 7–10% of the $Ru(bpy)_3^{2+}$ is excited, ~60% of the excited-state population decays to the ground state with an average lifetime of 55 ns. The quenching rate, therefore, appears to be considerably larger than those observed in sodium dodecyl sulfate below the critical micelle concentration for a similar ratio of [$Ru(bpy)_3^{2+*}$]:[$Ru(bpy)_3^{2+}$].[27b] We attribute this difference to the larger cluster sizes in the clay interlayer.

The origin of the ion-segregation process (either between interlayers or within interlayers) is unclear. Lagaly and Weiss have

(28) Self-quenching of excited $Ru(bpy)_3^{2+}$ also occurs in clays other than smectites. Thus, we have observed variations in emission kinetics with illumination intensity in kaolinite suspensions as well. The kaolinites are nonexpandable clays with a small cation-exchange capacity (cec) (2–5 meq/100 g). However, since the cations are located on the exterior surface and the particles are quite thick, the density of charge of the small exterior surface is not much smaller than that of montmorillonite or hectorite.[19] Hence, self-quenching due to appreciable buildup of $Ru(bpy)_3^{2+}$ concentration on kaolinite surfaces is possible. We could not carry out detailed studies of kaolinite suspensions because of severe problems with scattered light.

(29) Berkheiser, V. E; Mortland, M. M. *Clays Clay Miner.* **1977**, *25*, 105.

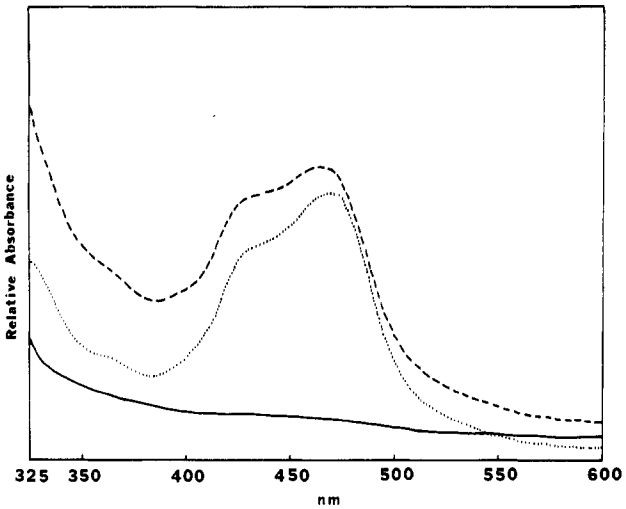


**Figure 7.** Absorption spectra in 2.5 g/L sodium hectorite: (—) $1 \times 10^{-4}$ M $Zn(bpy)_3^{2+}$; (···) $2 \times 10^{-5}$ M $Ru(bpy)_3^{2+}$; (- - -) $2 \times 10^{-5}$ M $Ru(bpy)_3^{2+}$ + $1 \times 10^{-4}$ $Zn(bpy)_3^{2+}$; $Ru(bpy)_3^{2+}$ and $Zn(bpy)_3^{2+}$ were premixed and then added to the clay suspension.

**TABLE I: Emission Kinetics Data[a] of Adsorbed $Ru(bpy)_3^{2+}$ [b] as a Function of $Zn(bpy)_3^{2+}$ Concentration**

| $10^5 \times [Zn(bpy)_3^{2+}]$,[c] M | $\alpha$[d] | $\tau_1$,[e] ns | $1 - \alpha$[f] | $\tau_2$,[g] ns | $I$[h] |
|---|---|---|---|---|---|
| 0 | 0.64 | 55 | 0.36 | 550 | 1 |
| 2 | 0.46 | 76 | 0.54 | 714 | 1.9 |
| 6 | 0.41 | 98 | 0.59 | 788 | 2.3 |
| 10 | 0.39 | 100 | 0.61 | 794 | 2.5 |

[a] Parameters obtained from a double-exponential fitting routine. [b] 0.02 mM $Ru(bpy)_3^{2+}$ in 2 g/L hectorite. [c] Added concentration of $Zn(bpy)_3^{2+}$. [d] Fraction of total emission attributable to fast component at time zero. [e] Lifetime of fast component. [f] Fraction of total emission attributable to slow component at time zero. [g] Lifetime of slow component. [h] Relative integrated luminescence yield.

shown that the charge distribution among different layers of smectites is nonuniform.[30] This has led Traynor et al. to speculate that segregation of ions may arise from a preference of the complex cations for interlayers of highest charge density.[31] However, segregation may also result from differences in sizes and solvation energies of the ions. Thus, after the first $Ru(bpy)_3^{2+}$ is incorporated between the clay layers, the energy to incorporate a second ion next to the first is lower than that to place it randomly in the particle. In addition, weak interactions between the $Ru(bpy)_3^{2+}$ ions may also be a contributing factor. In this connection the absorption spectral shifts shown in Figure 2a might be attributed to the large local concentrations of $Ru(bpy)_3^{2+}$ in the interlayers with interactions between bpy ligands of neighboring ions.[32]

*Luminescence of Clay/Ru(bpy)$_3^{2+}$, Quencher.* To pursue the problem of ion segregation further, we carried out flash photolytic studies of mixtures of $Ru(bpy)_3^{2+}$ and $Zn(bpy)_3^{2+}$ adsorbed in hectorite. The absorption spectra in colloidal sodium hectorite for $Zn(bpy)_3^{2+}$ (—), $Ru(bpy)_3^{2+}$ (···), and $Zn(bpy)_3^{2+}$ + $Ru(bpy)_3^{2+}$ (- - -) are shown in Figure 7. The emission kinetics measurements were carried out with a pulsed dye laser (excitation between 450 and 460 nm) so that $Zn(bpy)_3^{2+}$ is photochemically silent in our experiments. The luminescence decay profiles obtained for $2 \times 10^{-5}$ M $Ru(bpy)_3^{2+}$ (2.5 g/L hectorite) in the absence of $Zn(bpy)_3^{2+}$, and in the presence of $1 \times 10^{-4}$ M $Zn(bpy)_3^{2+}$, are shown in Figure 8, a and b, respectively. Both curves could be simulated by using the double-exponential fitting routine.

(30) Lagaly, G.; Weiss, A. *Proc. Int. Clay Conf. 1975* **1976**, 157–9.
(31) Traynor, M. F.; Mortland, M. M.; Pinnavaia, T. J. *Clays Clay Miner.* **1978**, *26*, 318.
(32) Absorption spectral shifts have also been observed in vessicular systems where the local concentrations of $Ru(bpy)_3^{2+}$ are also very high. Mau, A., personal communication.

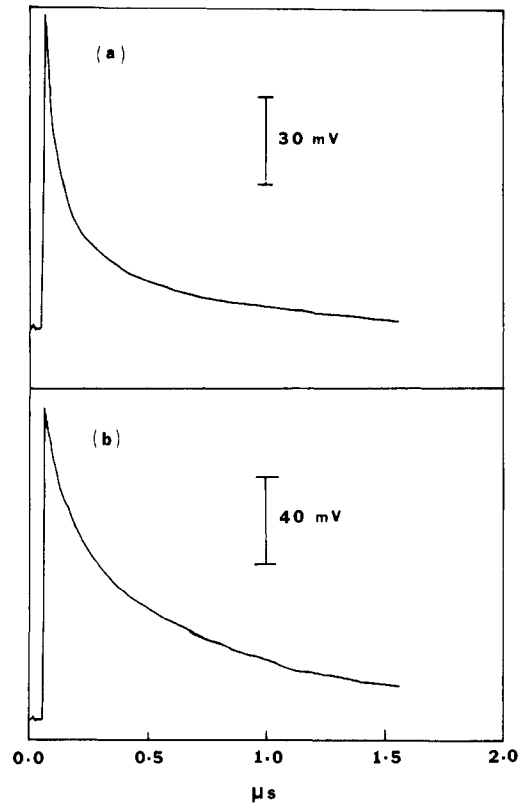


**Figure 8.** Emission decay profiles of (a) $2 \times 10^{-5}$ M $Ru(bpy)_3^{2+}$ in 2.5 g/L sodium hectorite and (b) $2 \times 10^{-5}$ M $Ru(bpy)_3^{2+}$ + $1 \times 10^{-4}$ M $Zn(bpy)_3^{2+}$ in 2.5 g/L sodium hectorite. The illumination conditions were identical and the excitation source was the 450-nm line from a nanosecond pulsed dye laser.

The emission kinetics measured for several concentrations of $Zn(bpy)_3^{2+}$ and values of the different parameters obtained from the simulation process are presented in Table I. The self-quenching rate can be seen to become progressively slower as the $Zn(bpy)_3^{2+}$ concentration is increased. For $Zn(bpy)_3^{2+}$ concentrations $\geq 6 \times 10^{-5}$ M (i.e., $[Zn(bpy)_3^{2+}]:[Ru(bpy)_3^{2+}] \geq 3$), the slower decay has a lifetime ($\tau$ = 788–794 ns) comparable to the natural radiative lifetime ($\tau$ = 800 ns) of $Ru(bpy)_3^{2+}$ in hectorite. The relative areas under the emission decay profiles correspond to the relative magnitudes of the total luminescence yield. Note that for $[Zn(bpy)_3^{2+}]:[Ru(bpy)_3^{2+}] = 1$, the observed luminescence yield is about twice the value obtained in the absence of $Zn(bpy)_3^{2+}$. The luminescence yield, however, does not increase proportionately for higher concentrations of $Zn(bpy)_3^{2+}$, and the decay profile remains multiphasic even when the $Zn(bpy)_3^{2+}$ concentration is as high as 0.1 mM ($[Zn(bpy)_3^{2+}]:[Ru(bpy)_3^{2+}] = 5$). These results, nevertheless, suggest that the diminished probability of self-quenching reflects a lowering of the effective concentration of $Ru(bpy)_3^{2+}$ in the interlayer. This is in sharp contrast to the negligible changes in effective concentration even for 10-fold variations in clay content. We presume, therefore, that on account of the similarity of $Ru(bpy)_3^{2+}$ and $Zn(bpy)_3^{2+}$, the clay particles are less likely to segregate these ions (Figure 6b), although the two together must still be completely adsorbed in a give interlayer before adsorption occurs in succeeding interlayers.

We have also probed the intercalation features of hectorite by carrying out quenching studies with viologens. The viologens chosen were methylviologen ($MV^{2+}$) and propylviologen sulfonate (PVS). The standard potentials of both couples $MV^{2+/+}$ and

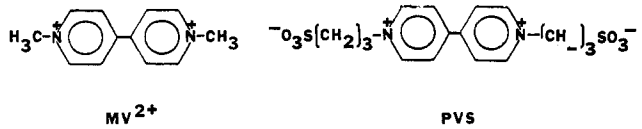

$PVS^{0/-}$ are similar (~−0.8 V vs. SCE) and both are efficient quenchers of the excited state of $Ru(bpy)_3^{2+}$ by an electron-transfer process (eq 1) in homogeneous solution.[33] The forward electron

$$Ru(bpy)_3^{2+*} + MV^{2+} \text{ (or PVS)} \rightarrow Ru(bpy)_3^{3+} + MV^{+} \text{ (or } PVS^{-}\cdot) \quad (1)$$

$$Ru(bpy)_3^{3+} + MV^{+}\cdot \text{ (or } PVS^{-}\cdot) \rightarrow Ru(bpy)_3^{2+} + MV^{2+} \text{ (or PVS)} \quad (2)$$

transfer is followed by the back-reaction shown in eq 2. The back-reaction rate is diffusion controlled in homogeneous solution, but can be slowed down in the presence of colloidal $SiO_2$, as demonstated by Willner et al.[33] The reduced viologens can be generated in substantial amounts (as evidenced by the appearance of a blue color), if $Ru(bpy)_3^{3+}$ is intercepted by the addition of a sacrificial donor, such as triethanolamine (TEOA).

The availability of two viologens with different net charges, but otherwise possessing similar properties, allowed us to study the quenching behavior in hectorite as a function of the quencher charge. Stern–Volmer plots obtained with the neutral viologen, PVS, as quencher were linear in clay-free solution (Figure 9A (●), $k_q = 9.5 \times 10^8$ $M^{-1}$ $s^{-1}$). The plots showed a distinct curvature in the colloidal system (○). We presume that the deviation from linearity results from weak adsorption of PVS on the hectorite surface. Similar deviations have been observed in studies with nitrobenzene and dimethylaniline as quencher molecules.[15] Since adsorption of PVS would increase its local concentration on the surface, the quenching rate constant, $k_q$, is presumably $<9.5 \times 10^8$ $M^{-1}$ $s^{-1}$. To prove that the quenching of adsorbed $Ru(bpy)_3^{2+*}$ emission is due to an electron-transfer reaction (eq 1), we carried out photochemical studies using TEOA as a sacrificial donor. TEOA reacts with $Ru(bpy)_3^{3+}$ and prevents the back-reaction, eq 2. The blue color of $PVS^{-}\cdot$ was indeed generated in these experiments, confirming that quenching occurs via electron transfer.[34] The rate of generation of $PVS^{-}\cdot$ was comparable in water and in hectorite suspension, in contrast to the dramatic increase in quantum yield which has been observed in the colloidal $SiO_2$ system.[35] Interestingly, no $PVS^{-}\cdot$ was formed in the colloidal clay system when EDTA was used instead of TEOA as a sacrificial donor, although EDTA is effective in a similar role in homogeneous solution. This indicates that EDTA does not have access to the clay interlayer.

The Stern–Volmer plot obtained for $Ru(bpy)_3^{2+}$–$MV^{2+}$ in water is shown in Figure 9B (●). The quenching rate constant was $3 \times 10^8$ $M^{-1}$ $s^{-1}$, in reasonable agreement with literature values.[36] Figure 9B also shows the Stern–Volmer plot for $Ru(bpy)_3^{2+}$–$MV^{2+}$ in colloidal hectorite (○). The effective concentration of $MV^{2+}$ was estimated on the basis of the knowledge that the density of clay is about 2 g/mL and the knowledge that all of the $MV^{2+}$ was adsorbed in the clay. From the plot we have calculated the quenching rate constant, $k_q$, as $<1.8 \times 10^6$ $M^{-1}$ $s^{-1}$. There is obviously a dramatic decrease in the quenching efficiency of $MV^{2+}$ when it is adsorbed in the clay. We do not believe that this peculiar behavior is due to any chemical inertness of adsorbed $MV^{2+}$.[38] Instead, we hypothesize that $MV^{2+}$ is unable to quench $Ru(bpy)_3^{2+}$ because these ions are spatially separated as a result of segregation in the clay layers (Figure 6c). To test our hypothesis we measured

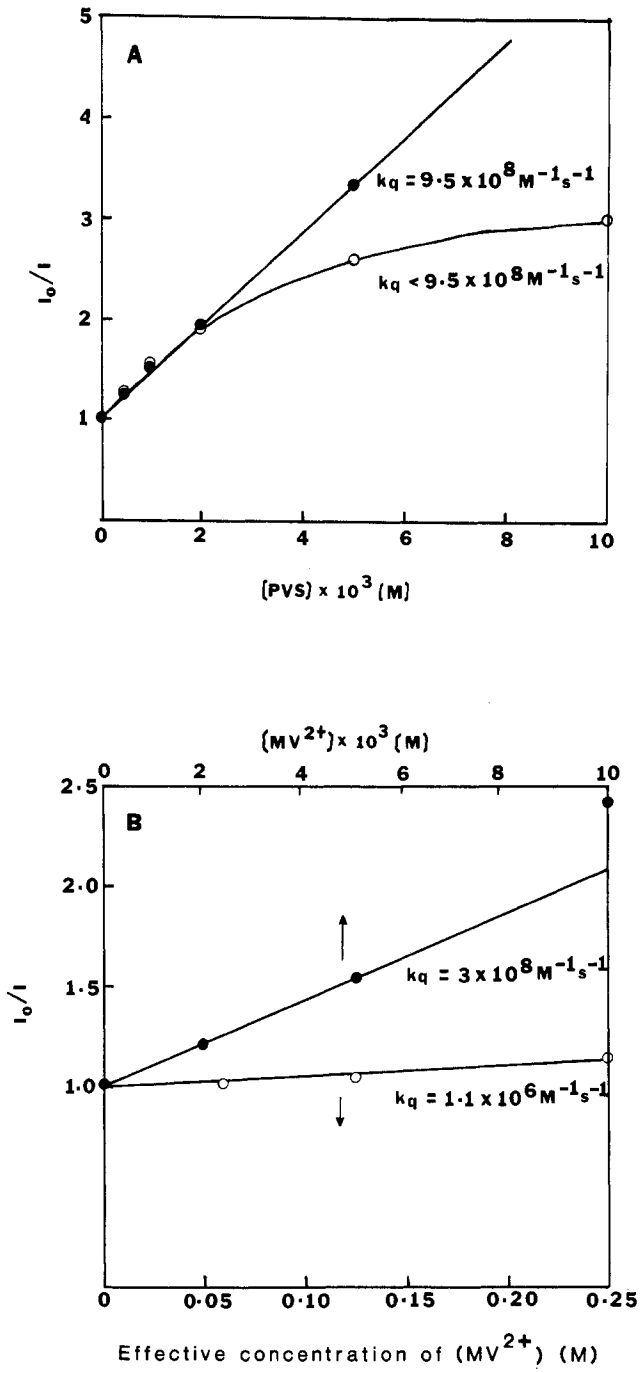


**Figure 9.** Steady-state Stern–Vollmer plots of $Ru(bpy)_3^{2+*}$ quenching in water (·) and in 2 gL sodium hectorite (○). (A) PVS and (B) $MV^{2+}$; $Ru(bpy)_3^{2+}$ ($2 \times 10^{-5}$ M) and the quencher ion were premixed and then added to the clay suspension.

the emission kinetics of $2 \times 10^{-5}$ M adsorbed $Ru(bpy)_3^{2+}$ in the absence and presence of $1 \times 10^{-4}$ M $MV^{2+}$. There was virtually no difference in their luminescence decay profiles. If $Ru(bpy)_3^{2+}$ and $MV^{2+}$ were randomly mixed in the clay interlayer and if the lack of quenching were due to other (inexplicable) reasons, we should have observed a substantial decrease in the self-quenching rate, as was the case in the $Ru(bpy)_3^{2+}$–$Zn(bpy)_3^{2+}$ system. Hence, the emission kinetics data support our hypothesis that $MV^{2+}$ and $Ru(bpy)_3^{2+}$ are segregated upon adsorption.

## Conclusions

One of the primary conclusions from these studies is that the local concentration of $Ru(bpy)_3^{2+}$ in the clay interlayers is very large (~$10^{-10}$ mol/cm$^2$ of surface area), even when the added concentration of $Ru(bpy)_3^{2+}$ is only 1–2% of the cation-exchange capacity. The high concentrations are achieved as a result of ion

(33) Willner, I.; Yang, J.-M.; Laane, C.; Otvos, J. W.; Calvin, M. *J. Phys. Chem.* **1981**, *85*, 3277.

(34) The excited-state electron-transfer reaction is exergonic by only 0.35 eV in aqueous solution. The ready occurrence of this reaction for adsorbed $Ru(bpy)_3^{2+}$ argues against any substantial shifts in the ground-state redox potential of $Ru(bpy)_3^{3+/2+}$.[14]

(35) Note that the hectorite interlayer is rather liquidlike.[14] We are currently pursuing similar experiments with kaolinite and illite where only the exterior surface is available for cation adsorption. In that respect these latter clays bear a close resemblance to the colloidal $SiO_2$ particles.

(36) (a) Gratzel, M.; Kiwi, J.; Kalyanasundaram, K. *Helv. Chim. Acta.* **1978**, *61*, 2720. (b) Darwent, J. R.; Kalyanasundaram, K. *J. Chem. Soc., Faraday Trans. 2* **1981**, *77*, 373.

(37) Rengasamy, P.; Van Assche, J. B.; Uytterhoeven, J. B. *J. Chem. Soc., Faraday Trans. 1* **1976**, *72*, 376.

(38) We have recently carried out bulk coulometry of $MV^{2+}$ adsorbed in colloidal dispersions of clay and our results indicate that reduction of $MV^{2+}$ occurs at potentials close to the $E^\circ$ value in solution.

segregation either between interlayers or within an interlayer. Due to the high local concentrations, very efficient self-quenching of $Ru(bpy)_3^{2+*}$ is observed under high intensity (pulsed laser) conditions. However, when $Zn(bpy)_3^{2+}$ is coadsorbed in hectorite, the effective self-quenching rate is dramatically reduced, presumably due to dilution of $Ru(bpy)_3^{2+}$ in the interlayer. On the other hand, no effect on the luminescence decay profile was observed when $Zn(bpy)_3^{2+}$ was replaced with $MV^{2+}$. Moreover, $MV^{2+}$ does not quench the excited state of $Ru(bpy)_3^{2+}$ (in hectorite suspension) even though such quenching is readily observed for the neutral viologen, PVS. We attribute these results to ion segregation; i.e., $MV^{2+}$ and $Ru(bpy)_3^{2+}$ are located in different regions of the clay interlayers.

Although self-quenching is presumed to occur via triplet–triplet annihilation,[26] the mechanistic details of the process remain largely unanswered. As previously mentioned, our preliminary results suggest that when only 7–10% of the $Ru(bpy)_3^{2+}$ is excited, ~60% of the excited molecules decay with an average lifetime of 55 ns. With a $D$ value of $5 \times 10^{-6}$ cm$^2$/s for $Ru(bpy)_3^{2+*}$, and assuming that two excited states interact to produce one, it is estimated that two out of three $Ru(bpy)_3^{2+*}$ would decay to the ground state within 55 ns,[39] in agreement with the 60% decay which is actually observed. However, in view of the close-packed nature of $Ru(bpy)_3^{2+}$ in the interlayer, it is questionable whether a diffusion coefficient value of $5 \times 10^{-6}$ cm$^2$/s, i.e., comparable to solution values, is reasonable in this instance.[40] On the other hand, self-quenching due to direct collisions of the initially formed triplet states is unlikely for smaller values of the diffusion coefficient, and alternative mechanisms for energy/electron[41] transfer would then have to be invoked. Further experiments to help elucidate the mechanistic details of the self-quenching process are currently in progress.[42]

*Acknowledgment.* We are very grateful to Dr. Steve Atherton for his invaluable assistance with the laser flash photolysis experiments. We are also grateful to Prof. W. H. Woodruff for providing the resonance Raman spectra, and to Keith Wilkins for his help with the single-photon counting measurements. We also acknowledge helpful discussions with Drs. Albert Mau and Cliff Carlin. The laser flash photolysis experiments were performed at the Center for Fast Kinetics Research at the University of Texas at Austin. The CFKR is supported jointly by the Biotechnology Branch of the Division of Research Resources of NIH (RR00886) and by the University of Texas at Austin. The support of this research by a grant from International Business Machines is gratefully acknowledged.

**Registry No.** $MV^{2+}$, 4685-14-7; PVS, 92220-37-6; $Ru(bpy)_3^{2+}$, 15158-62-0; $Zn(bpy)_3^{2+}$, 16571-18-9.

(39) For a diffusion coefficient of $5 \times 10^{-6}$ cm$^2$/s for $Ru(bpy)_3^{2+*}$ in the interlayer, it is estimated that the excited molecules can traverse an area, $A$, spanning $5.5 \times 10^{-13}$ cm$^2$ in 55 ns ($A = 2D$). For the situation where all cec sites in an interlayer are completely occupied by $Ru(bpy)_3^{2+}$, the average area/$Ru(bpy)_3^{2+}$ is calculated to be $\sim 1.25 \times 10^{-14}$ cm$^2$; i.e., 44 molecules are located within $5 \times 10^{-13}$ cm$^2$. Since only 7% of the molecules are excited following a laser flash, there are roughly three excited molecules within this area, at time zero.

(40) While it has previously been claimed that the environment in the interlayer is rather liquidlike,[14,15] a recent report[25] has arbitrarily put forward a value of $10^{-10}$ cm$^2$/s for the diffusion coefficient of $Ru(bpy)_3^{2+}$ adsorbed in clay. Note that a direct comparison of diffusion coefficients in the clay interlayer and in free solution is difficult since in the former case diffusion is restricted to a two-dimensional plane.

(41) From a consideration of energetics, triplet–triplet annihilation can occur both by energy transfer[27b] as well as by electron transfer (Sutin, N. *J. Photochem.* **1979**, *10*, 19.

(42) Atherton, S.; Ghosh, P. K.; Lynch, J.; Bard, A. J., work in progress.

# Surface Selection Rules for Surface-Enhanced Raman Spectroscopy: Calculations and Application to the Surface-Enhanced Raman Spectrum of Phthalazine on Silver

**M. Moskovits* and J. S. Suh**

*Department of Chemistry and Erindale College, University of Toronto, Toronto, Ontario, M5S 1A1 Canada*
*(Received: April 3, 1984)*

The "surface selection rules", i.e., the modification of the band intensities of a spectrum due to the proximity of the carrier to a surface, which are pertinent to surface-enhanced Raman are considered for the case of a molecule adsorbed on a metal sphere as a model. One concludes that there are three types of bands in the spectrum classed according to the Raman polarizability components which contribute strongly to them. Each type is characterized by its own SER excitation spectrum. It is also shown that in the spectral region between the bulk and surface plasma resonance frequencies of the sphere the electric field component parallel to the surface of the illuminated colloid particle may exceed the normal component. Calculations illustrating these points are presented as are experimental results obtained from the SER spectrum of phthalazine adsorbed on aqueous silver sol. The ratio of the intensities of $a_1$ modes and $b_2$ modes are shown to fit the ratio calculated on the basis of the electromagnetic model, provided one modifies the latter suitably to shift the surface plasma frequency to the red in order to take into account the effect colloid aggregation.

It is now a well-established fact that the absorption intensities of infrared modes of molecules adsorbed on flat metal surfaces are modified as a result of the presence of the surface so as to cause only those vibrational modes to be seen which have a nonvanishing component of the transition dipole moment normal to the surface.[1] One way of rationalizing this observation is by considering the s- and p-polarized electric field at the surface to be a superposition of an incident and a reflected field.[2] The s-polarized and p-polarized field strengths will therefore be proportional to $1 + r_s$ and $1 + r_p$, respectively, where the quantities $r_s$ and $r_p$ are the Fresnel coefficients. For most metals, $r_s$ approaches −1 while $r_p$ approaches unity in the infrared; hence, the former field polarization is greatly attenuated in that spectral region, while the latter is increased.

There is a region of the spectrum where precisely the opposite situation is expected, that is, where the tangential field strength exceeds the normal field component. The frequency where this

(1) Greenler, R. G. *J. Chem. Phys.* **1966**, *44*, 310; **1969**, *50*, 1963. Pearce, H. A.; Sheppard, N. *Surf. Sci.* **1976**, *59*, 205.

(2) Moskovits, M. *J. Chem. Phys.* **1982**, *77*, 4408.

0022-3654/84/2088-5526$01.50/0 © 1984 American Chemical Society